Self-diffusion in a periodic porous medium: A comparison of different approaches

David J. Bergman* and Keh-Jim Dunn
Chevron Petroleum Technology Company, P.O. Box 446, La Habra, California 90633-0446

Lawrence M. Schwartz
Schlumberger-Doll Research, Old Quarry Road, Ridgefield, Connecticut 06877-4108

Partha P. Mitra
AT&T Bell Laboratories, Murray Hill, New Jersey 07974
(Received 4 October 1994)

We compare two different approaches for computing the propagator for a particle diffusing in a fluid filled porous medium, where the pore space has a periodic structure and some absorption of the particle can occur at the pore-matrix interface. One of these approaches is based on computer simulations of a random walker in this structure, while the other is based on an explicit calculation of the diffusion eigenstates using a Fourier series expansion of the diffusion equation. Both methods are applied to the same nondilute model systems in order to calculate the wave-vector and time-dependent nuclear magnetization measured in pulsed-field-gradient–spin-echo experiments. When the physical parameters are confined to the range of values found in most systems of interest, good quantitative agreement is found between the two methods. However, as the interfacial relaxation strength, the time, or the wave vector becomes large, calculations based on eigenstate expansion are more stable and less subject to the sampling problems inherent in random walk simulations. In the absence of surface relaxation, our calculations are also used to test the results predicted by a recently proposed ansatz for the behavior of the diffusion propagator. Finally, a problem is identified and discussed regarding the relation between random walk and continuum diffusion treatments of interface absorption.

PACS number(s): 47.55.Mh, 05.60.+w, 07.57.Pt, 66.10.Cb

I. INTRODUCTION

Advances in measurement techniques, such as nuclear spin echo in the presence of a pulsed magnetic field gradient (PFGSE), have recently made possible detailed experimental studies of particle diffusion in some restricted geometries [1–4]. In parallel, a number of approaches have been developed for performing theoretical and numerical studies of diffusion in such geometries [5–12]. Two of these are notable in not being restricted to systems that are either dilute (i.e., a low concentration of obstacles to diffusion in an otherwise homogeneous medium) or have a very simple microstructure (e.g., isolated spherical pores). These are the method of random walker simulations [5,6,10,11] and the method of diffusion eigenstates in a periodic microstructure [12]. These approaches are totally different in all of their aspects and therefore it is of interest to compare their performance and find out under what conditions one of them might be preferable. Here we report on such a comparison. We also test the validity of a certain ansatz, proposed in Ref. [8], wherein a time-dependent diffusion coefficient, which is always useful for describing *long wavelength behavior*, is also used to characterize the *short wavelength behavior*.

Having specified the geometry of the porous medium, the PFGSE amplitude can be viewed as a function of the following parameters: the time t, the wave vector $\mathbf{k}$, the diffusion coefficient in the pore space D_0, and the interfacial absorption coefficient or relaxation strength ρ. In general, the calculations become easier as the magnitude of either t, $\mathbf{k}$, or ρ *decreases*. For example, as $\mathbf{k} \to \mathbf{0}$ the amplitude is determined by the effective time-dependent diffusion coefficient $D(t)$ and the two methods are found to yield essentially identical results over the entire range of t and ρ values studied. On the other hand, at larger $\mathbf{k}$ values, as either t or ρ becomes large, we find noticeable differences between the results obtained by the two methods. Generally these are cases where the calculated amplitude is quite small and the simulation technique is limited by statistical considerations. However, we find that within the experimentally accessible range of parameters, the two methods are in quite good agreement. In order to achieve this good agreement, we found that the precise relationship between the absorption parameters used in the two approaches had to be adjusted empirically. This is a result of some important subtleties in this problem, associated with the fact that the absorption is a *surface* rather than a *volume* process. While these issues were discussed in a one-dimensional context in Refs. [6,7], related problems that arise in higher dimensions were discovered in the course of this work and

*Permanent address: School of Physics and Astronomy, Raymond and Beverly Sackler Faculty of Exact Sciences, Tel Aviv University, Tel Aviv 69978, Israel.

are discussed here. Because these subtleties were not appreciated earlier, they were not dealt with in setting up the random walker algorithm which was used in the present calculations. That is why we had to resort to an empirical adjustment.

The remainder of this article is organized as follows. In Sec. II we present a brief summary of the basic theory of diffusion in the presence of interface absorption and of the two computational methods which were developed from the above mentioned approaches. In Sec. III we consider the application of these methods to a model porous medium comprised of spherical grains centered on the sites of a periodic simple cubic lattice. Here the grain radii may be chosen large enough that the grains overlap and the resulting porosity (i.e., the volume fraction occupied by the pore space) takes low values which are typical of many systems of experimental interest. In Sec. IV we discuss the relation between the continuum description of interface absorption and the implementation of this process in random walker simulations.

II. SUMMARY OF THE THEORY AND COMPUTATIONAL METHODS

All the information about self-diffusion in a restricted geometry is contained in the diffusion propagator $G(\mathbf{r},\mathbf{r}',t)$, which is the solution of the following mathematical problem:

$$\frac{\partial G}{\partial t} = D_0\nabla^2 G \quad \text{inside the pore space,} \tag{2.1}$$

$$G|_{t=0} = \delta^3(\mathbf{r}-\mathbf{r}'), \tag{2.2}$$

$$D_0\frac{\partial G}{\partial n} + \rho G = 0 \quad \text{at the pore-matrix interface.} \tag{2.3}$$

Here D_0 is the diffusion coefficient of the pore fluid and ρ is a coefficient which determines the rate of particle absorption at the obstacle surfaces.

For example, the PFGSE amplitude $M(\mathbf{k},t)$ is given by a double spatial Fourier transform of G (see, e.g., Ref. [8])

$$M(\mathbf{k},t) = \frac{1}{V_p}\int_{V_p} dV \int_{V_p} dV' G(\mathbf{r},\mathbf{r}',t)e^{-i\mathbf{k}\cdot(\mathbf{r}-\mathbf{r}')}. \tag{2.4}$$

Here V_p is the total volume of the pore space and the wave vector $\mathbf{k}$ is simply related to the value ∇H of the (uniform) magnetic field gradient and its duration δ

$$\mathbf{k} = \gamma\delta\nabla H, \tag{2.5}$$

where γ is the gyromagnetic ratio of the nuclear magnetic moment of the diffusing particles.

For the case of diffusion in a homogeneous fluid, G is given by

$$G(\mathbf{r},\mathbf{r}',t) = \left(\frac{1}{4\pi D_0 t}\right)^{3/2}\exp\left[-\frac{(\mathbf{r}-\mathbf{r}')^2}{4D_0 t}\right] \tag{2.6}$$

and $M(\mathbf{k},t)$ then has the simple form

$$M(\mathbf{k},t) = e^{-D_0 k^2 t}. \tag{2.7}$$

For diffusion in a restricted geometry, both G and M will depend on the detailed microstructure. This is reflected in the methods that will now be outlined for calculating these quantities.

The value of $M(\mathbf{k},t)$ at $\mathbf{k}=\mathbf{0}$ represents the total magnetization of the system and we will denote it by $M(t)$. For $\rho = 0$ it has the constant value 1, but for $\rho > 0$ it decays in time from $M(0) = 1$ to $M(\infty) = 0$. If we normalize $M(\mathbf{k},t)$ by dividing it by $M(t)$, then for small $\mathbf{k}$ the normalized value has the simple form [11]

$$\frac{M(\mathbf{k},t)}{M(t)} = e^{-D(t)k^2 t}. \tag{2.8}$$

This relation defines the bulk effective time-dependent diffusion coefficient $D(t)$, which then characterizes the behavior of the normalized PFGSE amplitude for small $\mathbf{k}$. The coefficient $D(t)$ decreases with increasing t and therefore tends to different finite limiting constants at very short and very long times

$$D(t) \longrightarrow \begin{cases} D_0 & \text{for } t \to 0 \\ D_e & \text{for } t \to \infty, \end{cases} \tag{2.9}$$

where D_e is the bulk effective stationary diffusion coefficient of the porous medium. The time-dependent diffusion coefficient $D(t)$ is easily calculated from values of $M(\mathbf{k},t)$ at small $\mathbf{k}$ vectors. It can also be calculated, even without knowing $M(\mathbf{k},t)$, from a knowledge of the mean square displacement of a diffusing particle $\langle[\delta\mathbf{r}(t)]^2\rangle$

$$\langle[\delta\mathbf{r}(t)]^2\rangle \equiv \frac{1}{M(t)}\frac{1}{V_p}\int_{V_p} dV \int_{V_p} dV'(\mathbf{r}-\mathbf{r}')^2 G(\mathbf{r},\mathbf{r}',t) = 6D(t)t. \tag{2.10}$$

While $D(t)$ is always a useful quantity for describing the *long wavelength* diffusion behavior, i.e., $M(\mathbf{k},t)$ at small $\mathbf{k}$, an ansatz has also been proposed wherein $D(t)$ is used to characterize $M(\mathbf{k},t)$ at *arbitrary values of* $\mathbf{k}$ [8]. For a porous medium with a *periodic microstructure*, that ansatz can be written as [see Eq. (9) of Ref. [8]]

$$M(\mathbf{k},t) \approx \frac{\sum_{\mathbf{g}} e^{-(\mathbf{k}-\mathbf{g})^2 D(t)t}|\theta_{\mathbf{g}}|^2}{\sum_{\mathbf{g}} e^{-\mathbf{g}^2 D(t)t}|\theta_{\mathbf{g}}|^2}. \tag{2.11}$$

Here the summation is over all the vectors $\mathbf{g}$ of the appropriate reciprocal lattice and

$$\theta_{\mathbf{g}} \equiv \int_{V_p} dV\, e^{-i\mathbf{g}\cdot\mathbf{r}} \tag{2.12}$$

is the Fourier expansion coefficient of the characteristic (or indicator) function of the pore space $\theta_p(\mathbf{r})$ (equal to 1 inside that pore space and to 0 elsewhere).

A. Diffusion simulations

Given a direct representation of the pore geometry, the PFGSE amplitude can be calculated by random walk simulations of diffusing particles [5]. Here we are concerned with an ordered system and the implementation of the random walk is quite straightforward. While these simulations take advantage of the periodicity of the system, it should be emphasized that the value of this technique is the relative ease with which it can be generalized to treat disordered systems.

In the algorithm used here, random walkers move through the pore space taking steps of fixed length ϵ. The step size ϵ is taken to be equal to $0.01a$, where a is the edge length of the simple cubic unit cell. (Several simulations were repeated with $\epsilon = 0.005a$ and showed no appreciable changes in the final results.) Walkers are launched from randomly chosen positions (x_0, y_0, z_0) within the pore space and, at each time step of size τ, advance from their current position (x_1, y_1, z_1) to a new position (x_2, y_2, z_2) on the surface of a sphere of radius ϵ:

$$x_2 = x_1 + \epsilon \sin\theta \cos\phi \ , \tag{2.13a}$$

$$y_2 = y_1 + \epsilon \sin\theta \sin\phi \ , \tag{2.13b}$$

$$z_2 = z_1 + \epsilon \cos\theta \ . \tag{2.13c}$$

We emphasize that $\cos\theta$ must be distributed uniformly in the range $(-1, 1)$ to ensure uniform coverage of the spherical surface. [Note that this is *not* equivalent to choosing θ uniformly in the interval $(0, \pi)$.] At prespecified time intervals each walker's contribution to the PFGSE amplitude is included in the sum [8]

$$M(\mathbf{k}, t) = \frac{1}{N} \sum_{n=1}^{N} \exp\left[i\mathbf{k} \cdot \{\mathbf{r}_n(t) - \mathbf{r}_n(t=0)\}\right] . \tag{2.14}$$

As the number of walkers N increases, the imaginary part of this expression becomes negligible compared to the real part. Alternatively, we could have calculated directly $P(\mathbf{r} \mid t)$ (the probability that a particle will diffuse a distance $\mathbf{r}$ in time t) and then Fourier transformed to get $M(\mathbf{k}, t)$. (Both approaches sometimes yield unphysical results [e.g., *negative* $M(\mathbf{k}, t)$ values] if the number of walkers is not large enough.)

The relation between the random walk parameters ϵ, τ, and the diffusion coefficient D_0 is

$$D_0 = \frac{\epsilon^2}{6\tau}, \tag{2.15}$$

since the diffusion process *in the bulk fluid* is accurately described by the three-dimensional Gaussian probability distribution of (2.6).

Implementation of the boundary condition (2.3) is, in principle, straightforward [5–7] as long as the absorption strength ρ is reasonably weak (as is the case in almost all experiments of interest). In the limit $\rho = 0$, we have *blind* reflection at the pore-grain interface: the walker returns to its attempt position and the clock advances by one time step τ. For $\rho \neq 0$, when a walker encounters the interface its magnetic polarization is wiped out (i.e., the walker is "killed") with probability γ (per unit time step τ), which is *proportional to* ρ for sufficiently small ϵ

$$A\gamma = \frac{\rho\epsilon}{D_0} + O\left(\left(\frac{\rho\epsilon}{D_0}\right)^2\right), \tag{2.16}$$

where A is a dimensionless proportionality coefficient of order 1 (in Refs. [5–7] a similar relation is given, but *without* the proportionality factor A). The exact relation between γ and ρ depends on details of the random walker algorithm in subtle ways, some of which were pointed out in Refs. [5–7], while others are discussed in Sec. IV below. The value of γ affects both $D(t)$ and $M(\mathbf{k}, t)$. Its most dramatic effect is on the total magnetization $M(\mathbf{k} = \mathbf{0}, t) \equiv M(t)$, which decays with time at an asymptotically exponential rate that is proportional to γ for small γ. In order to perform the comparisons of this paper we adjusted the value of A *for each sample* so as to achieve the same rate of decay for $M(t)$ in the two approaches. The values found in this way for A are shown in Table I.

Given specific values for the cube edge a and for D_0, we can easily convert the results of computer simulations into physical units. Returning to the PFGSE amplitude (2.14) we must now take account of the fact that the total magnetization $M(t)$ is decaying (i.e., that the number of walkers included in the sum is changing with time). Accordingly, we focus on the *normalized* PFGSE amplitude [8]

$$\frac{M(\mathbf{k}, t)}{M(t)} = \frac{1}{M(t)} \sum_{n} \exp\left[i\mathbf{k} \cdot \{\mathbf{r}_n(t) - \mathbf{r}_n(0)\}\right], \tag{2.17}$$

where the sum is now understood to include only those walkers surviving up to time t.

The simulations were also used to calculate $D(t)$ directly, without going through a calculation of $M(\mathbf{k}, t)$, by using the following implementation of (2.10):

$$6D(t)t = \frac{1}{M(t)} \sum_{n} [\mathbf{r}_n(t) - \mathbf{r}_n(0)]^2. \tag{2.18}$$

B. Fourier expansion of diffusion eigenfunctions

The diffusion propagator can always be expanded in terms of the diffusion eigenstates. When the microstruc-

TABLE I. Values of the proportionality factor A [see (2.16)], obtained by matching the diffusion simulation results for the total magnetization $M(t)$ to the corresponding results from the eigenstate expansion approach. Note that results for $\phi = 0.700$ are not discussed elswhere in this paper.

$\rho a/D_0$	ϕ=0.202	ϕ=0.4764	ϕ=0.700
0.2	1.49		1.39
0.3		1.37	
0.4	1.49		1.37
1.0	1.47	1.39	1.37

ture is periodic, the eigenfunctions have the Bloch-Floquet form

$$\phi_{n\mathbf{q}}(\mathbf{r})e^{i\mathbf{q}\cdot\mathbf{r}-\lambda_{n\mathbf{q}}t}, \tag{2.19}$$

where $\lambda_{n\mathbf{q}}$ is the eigenvalue, n is a band index, $\mathbf{q}$ is a wave vector in the first Brillouin zone of reciprocal space, and $\phi_{n\mathbf{q}}(\mathbf{r})$ is a periodic function. The periodic part of the eigenfunction satisfies the following equations:

$$\lambda_{n\mathbf{q}}\phi_{n\mathbf{q}} + D_0(\nabla + i\mathbf{q})^2\phi_{n\mathbf{q}} = 0 \text{ in the pore space,} \tag{2.20}$$

$$D_0\frac{\partial\phi_{n\mathbf{q}}}{\partial n} + \rho\phi_{n\mathbf{q}} = 0 \text{ at the pore-matrix interface.} \tag{2.21}$$

It can also be expanded in a Fourier series as

$$\theta_p(\mathbf{r})\phi_{n\mathbf{q}}(\mathbf{r}) = \sum_{\mathbf{g}}\tilde{\phi}_{n\mathbf{q}}(\mathbf{g})e^{i\mathbf{g}\cdot\mathbf{r}}. \tag{2.22}$$

The diffusion propagator can now be expanded as

$$G(\mathbf{r},\mathbf{r}',t) = \sum_{n,\mathbf{q}} e^{-\lambda_{n\mathbf{q}}t}\phi_{n\mathbf{q}}(\mathbf{r})\phi^*_{n\mathbf{q}}(\mathbf{r}')e^{i\mathbf{q}\cdot(\mathbf{r}-\mathbf{r}')}, \tag{2.23}$$

where the eigenfunctions are orthonormal in the volume of the pore space V_p, i.e.,

$$\int_{V_p} dV\phi^*_{n\mathbf{q}}\phi_{m\mathbf{q}} = \delta_{nm}. \tag{2.24}$$

The PFGSE amplitude has a particularly concise expression in terms of the Fourier expansion coefficients $\tilde{\phi}_{n\mathbf{q}}(\mathbf{g})$

$$M(\mathbf{k},t) = \frac{V}{\phi}\sum_n e^{-\lambda_{n\mathbf{q}}t}\,|\tilde{\phi}_{n\mathbf{q}}(\mathbf{g}_\mathbf{k})|^2\Big|_{\mathbf{q}=\mathbf{k}-\mathbf{g}_\mathbf{k}}, \tag{2.25}$$

where V is the total volume, $\phi \equiv V_p/V$ is the porosity, and $\mathbf{g}_\mathbf{k}$ is the reciprocal lattice vector that is closest to $\mathbf{k}$. For small $\mathbf{k}$ we just have $\mathbf{g}_\mathbf{k} = \mathbf{0}$ and $\mathbf{q} = \mathbf{k}$.

In the Fourier method, the eigenstates are found by solving a matrix eigenvalue problem, obtained from the differential equation (2.20) by using expansions such as (2.22). The transformation to a matrix eigenvalue problem is complicated by the fact that the boundary condition (2.21) must be taken into consideration. In the nonabsorbing case, when $\rho = 0$, this was done by reformulating (2.20) so that (2.21) is automatically satisfied [12]. Treatment of the $\rho \neq 0$ case is based upon the solution of the $\rho = 0$ case for the same microstructure: The $\rho \neq 0$ eigenstates are expanded in the $\rho = 0$ eigenstates and a new matrix eigenvalue problem is set up where the eigenvectors are the expansion coefficients [13]. Both types of matrix eigenvalue problems are solved by standard numerical methods and the results are then used in (2.25) to calculate $M(\mathbf{k},t)$. The time-dependent diffusion coefficient $D(t)$ is calculated from $M(\mathbf{k},t)$ at small $\mathbf{k}$ by using (2.8).

III. RESULTS AND COMPARISONS

The diffusion simulations always used a value for the proportionality coefficient A [see (2.16)] that was adjusted *separately for each sample* so as to give good agreement with the eigenstate expansion calculation of the total magnetization $M(t)$. Those values of A are shown in Table I and they are all in the range 1.37–1.49. In Sec. IV below we present an argument, which was produced by hindsight (i.e., after completion of the simulations), that may justify a value $A \approx 1.5$. We note, however, that while $M(t)$ itself is very sensitive to the value of A, we found that the normalized PFGSE amplitude $M(\mathbf{k},t)/M(t)$ is quite insensitive to that value. Therefore the results that we got for $M(\mathbf{k},t)/M(t)$ would be unchanged if we used $A = 1.5$ instead of the values from Table I.

In Fig. 1 we examine the general trends to be expected when the relaxation strength ρ is turned on in a simple cubic array of spherical obstacles that are just touching ($\phi = 0.4764$). The curves shown here for the PFGSE amplitude ratio $M(\mathbf{k},t)/M(t)$ were computed by the eigenstate expansion; the same trends are evident in the simulation results. In some sense, the most striking feature of these curves is how little the values of $M(\mathbf{k},t)/M(t)$ change as ρ is increased. In this connection we note that the effective pore diameter is somewhat smaller than the cube edge a, so that even the case shown here, where $\rho a/D_0 = 1$, is still within the fast diffusion or small ρ regime. Generally, the effects of surface relaxation become stronger as t increases. When t is large enough that we have well defined quasidiffraction peaks at $\mathbf{k}$ equal to any reciprocal lattice vector, the values of $M(\mathbf{k},t)/M(t)$ at the minima and maxima all increase with increasing ρ, while the location of these features in $\mathbf{k}$ space remains unchanged.

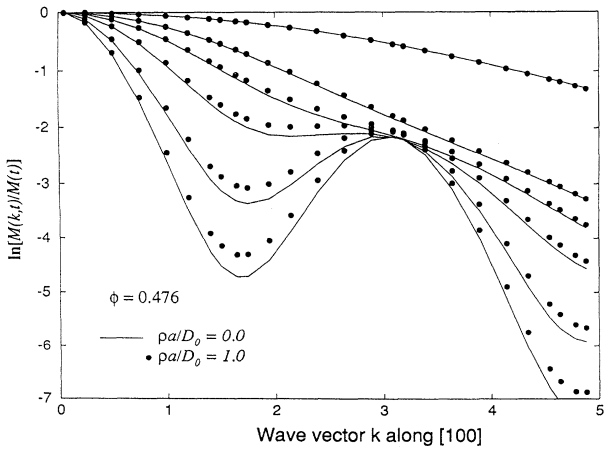

FIG. 1. For the case of touching spheres ($\rho = 0.4674$), calculations of $M(\mathbf{k},t)/M(t)$ based on the eigenstate expansion are shown for $\rho = 0$ and $\rho a/D_0 = 1$. Results are presented for six values of t corresponding to 0.67, 3.33, 6.67, 13.33, 26.67, and 40 msec. Here we take the cube edge to be equal to 10 μm and $D_0 = 2.5\ \mu\text{m}^2/\text{msec}$.

In Fig. 2 we compare the results of eigenstate expansion and diffusion simulation for $M(\mathbf{k},t)$ in the case $\rho = 0$. Here we consider the case of touching spheres ($\phi = 0.476$) and a case of overlapping spheres ($\phi = 0.202$) [14]. In both cases the two sets of results are in good agreement over a range of $\mathbf{k}$ values which includes the first quasidiffraction peak. We note that the diffraction peaks are considerably lower, even though they are more pronounced above the background, in the case of the higher porosity sample. Physically, this reflects the fact that $D(t)$ *decreases* with decreasing ϕ, at least in the case of an array of spherical obstacles [12,13]. This behavior can also be tied in with a consideration of the average probability density that a diffusing particle returns to its point of origin at the time t. When $\rho = 0$, this quantity is given by

$$\frac{1}{V_p}\int_{V_p} dV\, G(\mathbf{r},\mathbf{r},t) = \int \frac{d^3k}{(2\pi)^3}\, M(\mathbf{k},t). \qquad (3.1)$$

Intuitively, we can expect this quantity to increase with decreasing ϕ since it usually becomes more difficult for the particle to move away from its point of origin.

It is also of interest to compare the present calculations with the simple ansatz proposed in Ref. [8]. In Fig. 3 we see that, for $\rho = 0$, this ansatz leads to results which are qualitatively reasonable, although the depth and sharpness of the quasidiffraction minima is overestimated, as are their locations in $\mathbf{k}$ space.

In Fig. 4 we compare eigenstate expansion results with those obtained from diffusion simulation for $M(\mathbf{k},t)/M(t)$ at two nonzero values of ρ and at $\phi = 0.202$. Figure 4(a) shows a weak relaxation (fast diffusion, $\rho a/D_0 = 0.2$) case, where the two methods evidently yield very similar results. Figure 4(b) shows an intermediate relaxation strength case ($\rho a/D_0 = 1$), where somewhat greater differences appear between the two sets of data, especially at the longest time for which results are plotted.

One point worth noting in connection with Figs. 1–4 is the fact that the two techniques yield essentially identical results in the long wavelength limit $\mathbf{k} \to \mathbf{0}$ and also at

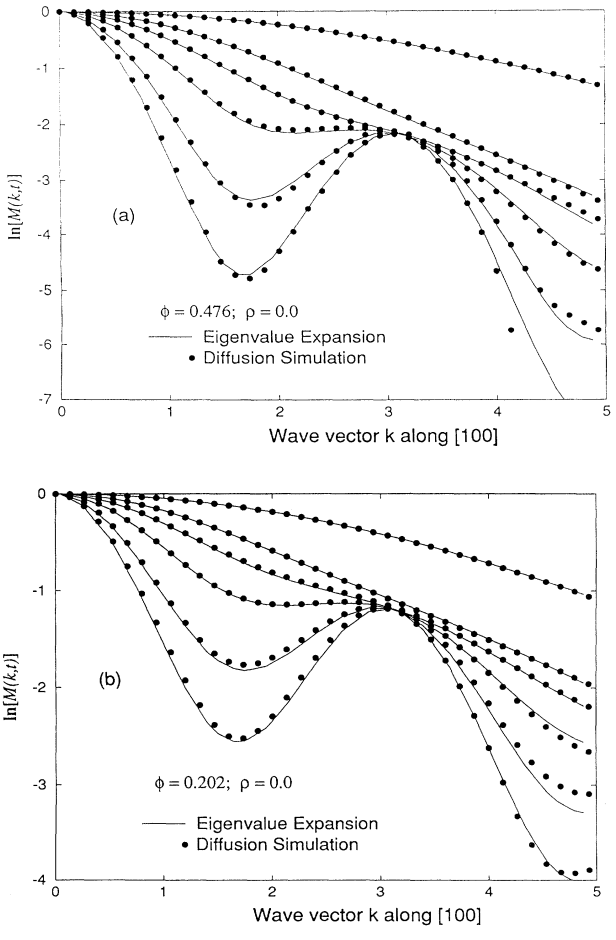

FIG. 2. Eigenstate expansion and diffusion simulation results for $M(\mathbf{k},t)$ are compared in the case $\rho = 0$ (a) for touching spheres ($\phi = 0.4674$) and (b) for overlapping spheres ($\phi = 0.202$), with $t = 0.67 \to 40.0$ msec.

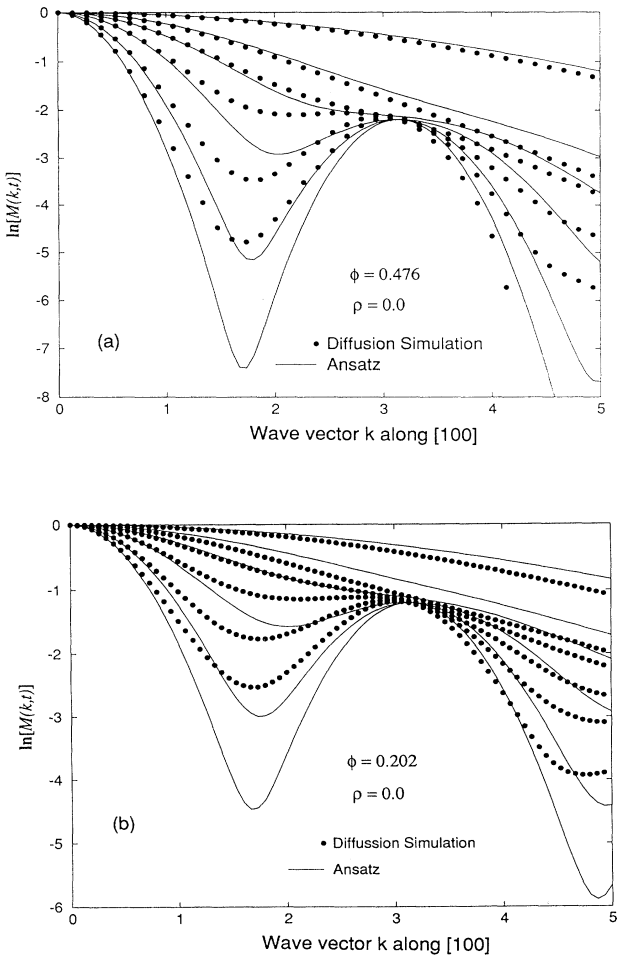

FIG. 3. Results for $M(\mathbf{k},t)/M(t)$ at $\rho = 0$ based on the ansatz (2.11), compared with results of the diffusion simulation (a) for $\phi = 0.4674$ and (b) for $\phi = 0.202$.

early times for all **k**. The quality of this agreement at small **k** is not evident in these figures, due to insufficient detail at small **k**, but it emerges quite convincingly when one plots $D(t)/D_0$ as calculated by the two methods. This is shown in Fig. 5 for the two porosities $\phi = 0.4764$ and 0.202 and for $\rho a/D_0 = 0$, 1.

Note that the results shown in Fig. 4 cover a more limited range of times than those shown in Fig. 1. We have limited our attention to times for which the total magnetization $M(t)$ has decayed to no less than 5% of its original value. Typically, this is the range of experimental interest. For longer times, the simulations become very time consuming because so few walkers survive that it is difficult to achieve an acceptable level of statistical accuracy. In addition, it should be noted that, even in the $\rho = 0$ case, the simulations become less accurate at long times and large **k** values. For example, in order to faithfully describe the diffraction minima it is necessary to compute some very small numbers with a high degree of accuracy and this requires that a prohibitively large number of walkers be simulated. For the totality of these reasons, we have appropriately limited the time ranges for which results are presented in Figs. 2–4. By contrast, the eigenstate expansion can easily treat both long times and large wave vectors; in fact, the longer the time the more accurate the results. Clearly, in ordered systems this technique is more dependable and less time consuming than diffusion simulation, but over the range of principal interest the two techniques yield similar results and with comparable quality. On the other hand, random walker simulation is still the only method available for studying self-diffusion in a nondilute, disordered system.

IV. THE RELATION BETWEEN γ AND ρ

The continuum description of microstructure restricted diffusion (i.e., diffusion in a porous medium) in the pres-

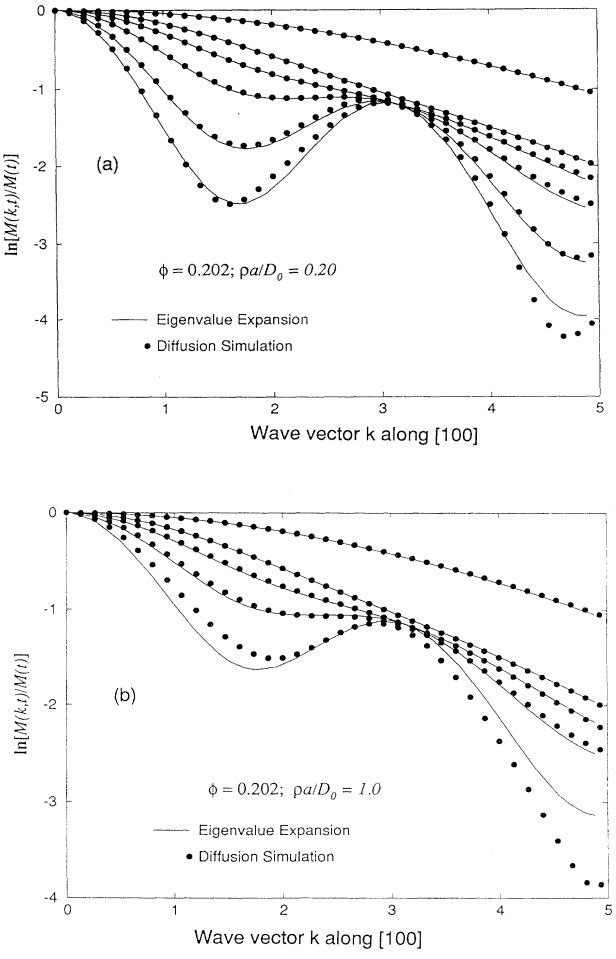

FIG. 4. Results for $M(\mathbf{k},t)/M(t)$ based on the eigenstate expansion and on diffusion simulations are compared for two values of the relaxation strength ρ. In (a) $\rho a/D_0 = 0.20$ and $t = 0.67 \rightarrow 40$ msec, while in (b) $\rho a/D_0 = 1.0$ and $t = 0.67 \rightarrow 26.67$ msec. In both sets of calculations $\phi = 0.202$.

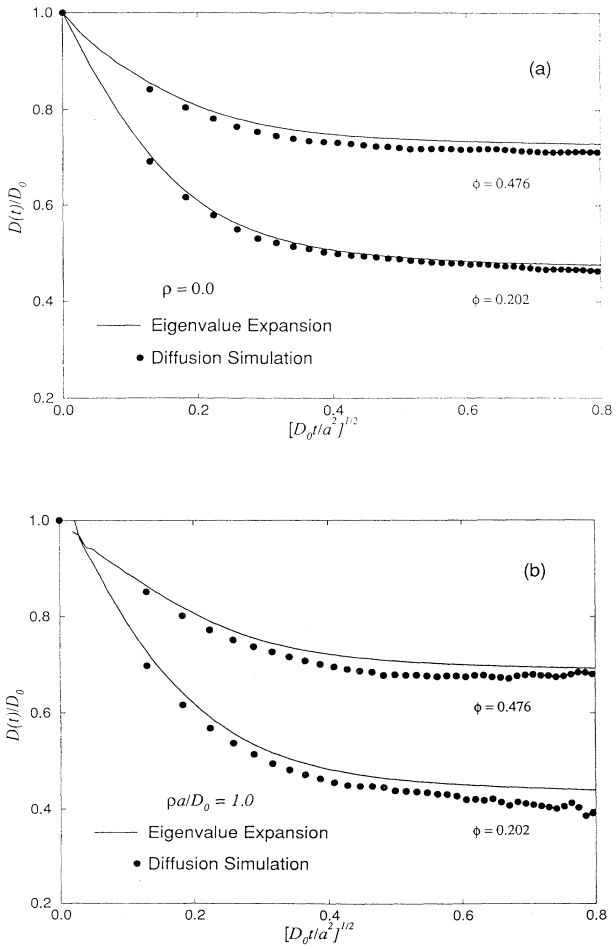

FIG. 5. Results for $D(t)/D_0$ based on the eigenstate expansion and on diffusion simulations are compared for two values of the relaxation strength ρ at the two porosities $\phi = 0.4764$ and 0.202. In (a) $\rho = 0$, while in (b) $\rho a/D_0 = 1.0$.

ence of interface absorption is unique and given by (2.1)–(2.3). By contrast, there are many different ways of constructing a discrete random walker algorithm to approximate this process. A necessary requirement is that as the size of the time step τ and/or that of the spatial step ϵ tend to 0, the discrete algorithm should tend to the continuum description. The presence of interface absorption introduces subtleties into this limit process which have to do with the absorption being a *surface phenomenon.*

This is easiest to appreciate in the case of an algorithm that differs from the one used in this work. In that algorithm, the walker can only advance in space by steps of $\pm\epsilon$ along *fixed coordinate axes.* This effectively discretizes space into a simple cubic lattice of available sites with a unit cell edge ϵ. When the walker reaches a surface site and attempts to cross to the other side, it either dies with probability γ or stays put at the surface site for one time step. The problem with this algorithm is that it really approximates the true surface by a set of right angled corners in those ϵ^3 cells which it intersects. This is illustrated in Fig. 6(a), where the (curvilinear) triangle ABC represents the intersection of the smooth interface with such a lattice. The algorithm effectively replaces that triangular section by the three right angled (curvilinear) triangles a,b,c which lie in planes that are perpendicular to the coordinate axes. The total area of those three triangles is always greater than the area of ABC and therefore the effective rate of surface absorption produced in the simulation is enhanced by a factor equal to the ratio of areas $(a+b+c)/ABC$. If we let ϵ tend to 0, this ratio will tend to a constant that depends on the local orientation of the interface with respect to the fixed coordinate axes and is usually greater than 1. Its average value for a spherical surface can be found by first considering the ratio

$$\frac{c}{ABC} = |\mathbf{n}\cdot\mathbf{e}_z| \equiv |\cos\theta|, \tag{4.1}$$

where $\mathbf{n}$ is a unit vector that is perpendicular to the surface section ABC and $\mathbf{e}_z$ is a unit vector along the z axis. The average of this ratio over a spherical surface is thus given by

$$\left\langle \frac{c}{ABC} \right\rangle = \frac{1}{4\pi}\int d\Omega\,|\cos\theta| = \frac{1}{2}. \tag{4.2}$$

Obviously, the other two ratios a/ABC and b/ABC have the same average values and therefore

$$\left\langle \frac{a+b+c}{ABC} \right\rangle = \frac{3}{2}. \tag{4.3}$$

For a system of nonoverlapping spherical obstacles, one could argue that this would be the correct value of the proportionality factor A in (2.16), if one were using this algorithm.

Since the algorithm used here is different, we attempted to find the appropriate relation between γ and ρ by focusing upon the following question: What is the *average* probability $\langle P_d\rangle$ for the walker to be dead at time $t=\tau$ if at time $t=0$ it was at any point that is within a distance ϵ from a *flat surface*?

That probability can easily be calculated from the random walker algorithm by noting that the probability for the walker to be dead at time τ is nonzero only if at time 0 its distance z from the surface was less than ϵ. If we draw a sphere of radius ϵ around the $t=0$ position of the walker, then the intersection of that sphere with the flat surface subtends a solid angle denoted by $\Omega(z)$ [see Fig. 6(b)], and the probability that the walker is dead at time τ is given by

$$P_d(z) = \frac{\Omega(z)}{4\pi}\gamma = \frac{1}{2}\left(1-\frac{z}{\epsilon}\right)\gamma. \tag{4.4}$$

The *average* probability that it is dead is therefore

$$\langle P_d\rangle = \frac{1}{\epsilon}\int_0^\epsilon dz P_d(z) = \frac{\gamma}{4}. \tag{4.5}$$

That probability can also be calculated from the continuum picture of diffusion by solving (2.1)–(2.3) and calculating the integral

$$\langle P_d\rangle = 1 - \frac{1}{\epsilon}\int_0^\epsilon dz \int_{z'>0} dV' G(\mathbf{r},\mathbf{r}',\tau). \tag{4.6}$$

For a flat boundary, G is a product of three one-dimensional propagators, two of which are free propagators [i.e., one-dimensional versions of (2.6)] while the third includes the effects of the boundary and can also be calculated in closed form (in terms of error functions). The integration finally leads to

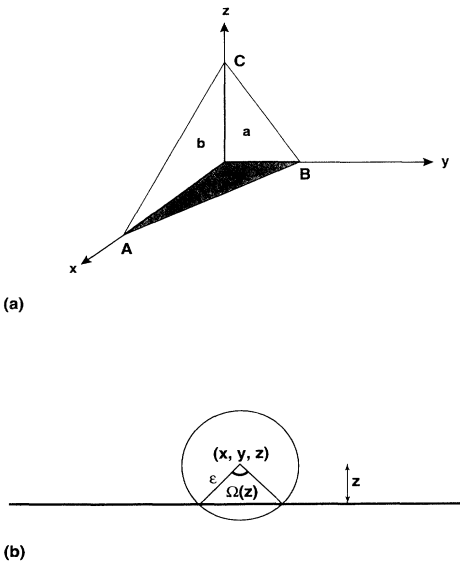

FIG. 6. (a) Illustration of the surface area enhancement that results from a discretization of space in a random walker simulation. (b) Illustration of the configuration used to calculate the probability for the random walker to die using the random walker algorithm of Sec. II A and the continuum diffusion picture.

$$\langle P_d \rangle = \frac{\rho\tau}{\epsilon}\left[1 - i^2\mathrm{erfc}\left(\sqrt{\frac{3}{2}}\right)\right] + O\left(\left(\frac{\rho\tau}{\epsilon}\right)^2\right)$$
$$\approx \frac{\rho\epsilon}{6D_0} \times 0.96, \tag{4.7}$$

where $i^2\mathrm{erfc}(x)$ is a twice iterated integral of $\mathrm{erfc}(x)$ [15] and where we used the relation $6D_0\tau = \epsilon^2$ [see (2.15)].

Equating the two expressions for $\langle P_d \rangle$ we immediately get

$$\frac{3/2}{0.96}\gamma = \frac{\rho\epsilon}{D_0}, \tag{4.8}$$

i.e., $A \approx 1.04 \times 3/2$. This is remarkably close to the value $A = 3/2$ that we found for the previous algorithm. It is also quite close to the values that we found empirically by fitting the decay rates for $M(t)$—see Table I.

Finally, we would like to point out that for both of the algorithms which we considered in this section, the actual local probability for the walker to die, as calculated by solving the differential equation, is not a constant. In the case of the first algorithm it depends on the *local orientation* of the interface. In the case of the second algorithm it depends on the actual distance from the walker to the nearest section of interface and should be calculated from $G(\mathbf{r}, \mathbf{r}', \tau)$. This observation suggests an alternative approach to the inclusion of surface absorption effects in random walker simulations, in which the discrete probability of dying is assigned a value that depends upon local conditions and reflects the details of the algorithm.

[1] P.T. Callaghan, A. Coy, D. MacGowan, K.J. Packer, and F.O. Zelaya, Nature **351**, 467 (1991).

[2] P.T. Callaghan, D. MacGowan, K.J. Packer, and F.O. Zelaya, Magn. Reson. Imaging **9**, 663 (1991).

[3] P.T. Callaghan, A. Coy, T.P.J. Halpin, D. MacGowan, K.J. Packer, and F.O. Zelaya, J. Chem. Phys. **97**, 651 (1992).

[4] P.T. Callaghan, *Principles of Nuclear Magnetic Resonance Microscopy* (Oxford University Press, Oxford, 1991); this book describes most of the relevant experimental and theoretical research in the field of NMR in porous media which was done before 1990, including references.

[5] J.R. Banavar and L.M. Schwartz, in *Molecular Dynamics in Restricted Geometries*, edited by J. Klafter and J.M. Drake (Wiley, New York, 1989), p. 273.

[6] D.J. Wilkinson, D.L. Johnson, and L.M. Schwartz, Phys. Rev. B **44**, 4960 (1991).

[7] K.S. Mendelson, Phys. Rev. B **47**, 1081 (1993).

[8] P.P. Mitra, P.N. Sen, L.M. Schwartz, and P. Le Doussal, Phys. Rev. Lett. **68**, 3555 (1992).

[9] P.P. Mitra and P.N. Sen, Phys. Rev. B **45**, 143 (1992).

[10] P.P. Mitra, P.N. Sen, and L.M. Schwartz, Phys. Rev. B **47**, 8565 (1993).

[11] P.N. Sen, L.M. Schwartz, P.P. Mitra, and B.I. Halperin, Phys. Rev. B **49**, 215 (1994).

[12] D.J. Bergman and K.J. Dunn, Phys. Rev. B **50**, 9153 (1994).

[13] D.J. Bergman and K.J. Dunn, following paper, Phys. Rev. E **51**, 3401 (1995).

[14] In order to connect between the time scales of the two computational methods we use the identity $D_0 t/a^2 = N\epsilon^2/(6a^2)$, where N is the number of random walk time steps. Thus, with $\epsilon/a = 0.01$, we have $t = 10^{-4}Na^2/(6D_0)$. Taking $a = 10$ μm and $D_0 = 2.5$ μm^2/msec we get the following correspondences: $N = 1000$ ($t = 0.67$ msec), $N = 5000$ ($t = 3.33$ msec), $N = 10\,000$ ($t = 6.67$ msec), $N = 20\,000$ ($t = 13.33$ msec), $N = 40\,000$ ($t = 26.67$ msec), and $N = 60\,000$ ($t = 40.0$ msec).

[15] *Handbook of Mathematical Functions*, edited by M. Abramowitz and I.A. Stegun (Dover, New York, 1972), Chap. 7.

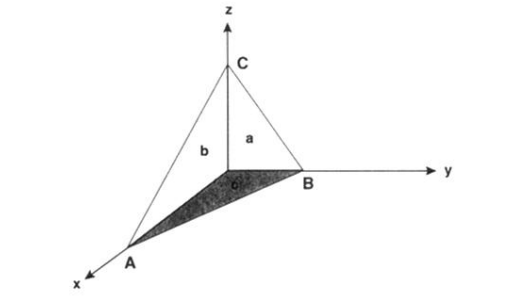

(a)

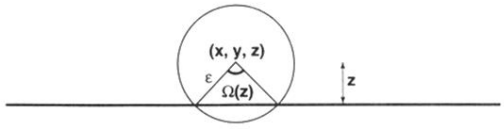

(b)

FIG. 6. (a) Illustration of the surface area enhancement that results from a discretization of space in a random walker simulation. (b) Illustration of the configuration used to calculate the probability for the random walker to die using the random walker algorithm of Sec. II A and the continuum diffusion picture.